

Direction dependence of cosmological parameters due to cosmic hemispherical asymmetry

Suvodip Mukherjee, Pavan K. Aluri, Santanu Das, Shabbir Shaikh and Tarun Souradeep

Inter University Centre for Astronomy and Astrophysics
Post Bag 4, Ganeshkhind, Pune-411007, India

E-mail: suvodip@iucaa.in, aluri@iucaa.in, santanud@iucaa.ernet.in,
shabbir@iucaa.in, tarun@iucaa.in

Abstract. Persistent evidence for a cosmic hemispherical asymmetry in the temperature field of cosmic microwave background (CMB) as observed by both WMAP as well as PLANCK increases the possibility of its cosmological origin. Presence of this signal may lead to different values for the standard model cosmological parameters in different directions, and that can have significant implications for other studies where they are used. We investigate the effect of this cosmic hemispherical asymmetry on cosmological parameters using non-isotropic Gaussian random simulations injected with both scale dependent and scale independent modulation strengths. Our analysis shows that A_s and n_s are the most susceptible parameters to acquire position dependence across the sky for the kind of isotropy breaking phenomena under study. As expected, we find maximum variation arises for the case of scale independent modulation of CMB anisotropies. We find that scale dependent modulation profile as seen in PLANCK data could lead to only 1.25σ deviation in A_s in comparison to its estimate from isotropic CMB sky.

Contents

1	Introduction	1
2	BipoSH representation of SI violation	2
3	Simulations	3
4	Assessing directional dependence of cosmological parameters	4
5	Conclusion	8
A	Local Variance Estimator	10

1 Introduction

Unprecedented quality of measurements of cosmic microwave background (CMB) temperature and polarization fields by several missions in the last few decades have significantly improved our understanding of the universe. The measured temperature anisotropy by WMAP [5] and PLANCK [1–4] is well explained by the minimal Λ CDM model. However, these missions also revealed an unforeseen signal that violates one of the fundamental pillars of cosmology viz., statistical isotropy (SI) of the cosmos. This isotropy violating signal in the CMB temperature field, known as cosmic hemispherical asymmetry (CHA), was detected at about 3σ significance in the clean CMB maps from WMAP [6, 7] as well as PLANCK [8, 9] data. It implies that the hemisphere centered at the direction, $\hat{p} = (l, b) = (228^\circ, -18^\circ)$ in Galactic coordinates [8, 9], possess enhanced temperature fluctuations, and correspondingly suppressed fluctuations in the opposite hemisphere. Several other analysis using WMAP and PLANCK data have also confirmed this effect [10–14]. The detection of this signal in both WMAP and PLANCK data reduces its chance of arising from an unknown systematic. As a result, it is important to understand its origin, and its implication to other observational windows of cosmology. Several models have been proposed in order to incorporate this effect [15, 17–32], and many of them also predict the likely signatures perceived in polarization data as a consequence.

The cosmological origin of this signal will affect the cosmological parameters and can lead to direction dependence in the derived parameters. As a result, the cosmological parameters obtained from different partial sky missions may contradict each other, and can be a source of tension between different data sets. Hence it is important to study the implications of this SI violation phenomena on cosmological parameters. Recently, an interesting study of this kind was carried out by Axelsson et al. [33] using WMAP 9 year data. However unknown systematics from foreground contaminations, masking or instrumental beam can conceal the complete effects of CHA. As a result, it is important to investigate the extent to which cosmological parameters are susceptible to the change due to the cosmological origin of this anomaly from ideal simulations. The cosmological parameters estimated from a SI and the corresponding statistically non-isotropic (nSI) realization produced from the same initial seed of the Gaussian distribution helps to estimate the variation of cosmological parameters with direction, and can capture the complete effect of CHA. Effects of different scale dependencies of dipole power asymmetry can also be investigated from our analysis.

We study the implication of CHA on cosmological parameters using ideal nSI simulations, which are free of foreground contamination, instrumental noise or asymmetric beam. An estimation of cosmological parameters from these simulations in different directions of the sky can shed light on the maximum possible variation that can be expected in these cosmological parameters due to CHA. These results can be compared with any future analysis of direction dependent cosmological parameters to carefully infer such a dependence in them, which might otherwise be possibly connected to systematics.

This paper is organized as follows. In section 2, we briefly review the Bipolar Spherical Harmonic (BipoSH) framework, a well suited language to quantify SI violation, that we use in this analysis. In section 3, we describe the procedure used to generate the simulations for our study. Results on estimation of cosmological parameters from different non-overlapping patches of the sky and conclusions are presented in section 4 and 5 respectively.

2 BipoSH representation of SI violation

The temperature and polarization field of CMB can be expressed as

$$X(\hat{n}) = \sum_{lm} X_{lm} Y_{lm}(\hat{n}); \quad X = T, E, B, \quad (2.1)$$

where, $Y_{lm}(\hat{n})$ are the Spherical Harmonics (SH) along the direction \hat{n} . The two point correlation function $\langle X_{lm} X_{l'm'}^* \rangle$ of temperature or polarization field can be expanded in the tensor product basis of two SH spaces as

$$K_{lm'l'm'} \equiv \langle X_{lm} X_{l'm'}^* \rangle = \sum_{JN} A_{ll'|XX'}^{JN} (-1)^{m'} C_{lml-m'}^{JN}, \quad (2.2)$$

where $A_{ll'}^{JN}$ are the BipoSH coefficients introduced in CMB analysis by Hajian & Souradeep [34, 35], and $C_{lml'm'}^{JN}$ are the Clebsch-Gordan coefficients. Under the assumption of statistical isotropy, the covariance matrix is diagonal i.e., the only non-vanishing coefficients are $A_{ll}^{00} = (-1)^l \sqrt{2l+1} C_l$ corresponding to $J = 0, N = 0$, where C_l is the familiar angular power spectrum. For the case of nSI CMB sky, off-diagonal terms of the covariance matrix are also non-zero, which in turn lead to non-zero BipoSH coefficients for $J > 0$.

The observed CHA can be modelled as [36, 37]

$$\tilde{T}(\hat{n}) = T(\hat{n})(1 + \alpha \hat{p} \cdot \hat{n}), \quad (2.3)$$

where $T(\hat{n})$ and $\tilde{T}(\hat{n})$ are the unmodulated and modulated CMB anisotropies in the sky direction \hat{n} . α is the modulation strength and \hat{p} denotes the direction of modulation field. In our analysis, we also consider the modulation field to be scale dependent $\alpha \equiv \alpha_l$ to mimic the observation by WMAP [6, 7] and PLANCK [8, 9]. This model generates only $J = 1$ BipoSH coefficients given as [8, 25]

$$A_{ll+1|TT}^{1N} = \mathcal{M}^{1N} [C_l^{TT} + C_{l+1}^{TT}] \frac{\Pi_{ll+1}}{\sqrt{4\pi}\Pi_1} C_{l0l+10}^{10}, \quad (2.4)$$

where \mathcal{M}^{1N} are the SH coefficients of the modulation field $\mathcal{M}(\hat{n}) = \alpha \hat{p} \cdot \hat{n}$, $\Pi_{l_1 l_2 \dots} = \sqrt{(2l_1+1)(2l_2+1)\dots}$ and C_l^{TT} is the temperature angular power spectra. The modulation amplitude α is related with \mathcal{M}^{1N} by the relation $\alpha = 1.5 \sqrt{\frac{\sum_N |\mathcal{M}^{1N}|^2}{3\pi}}$. In Fig. 1 we

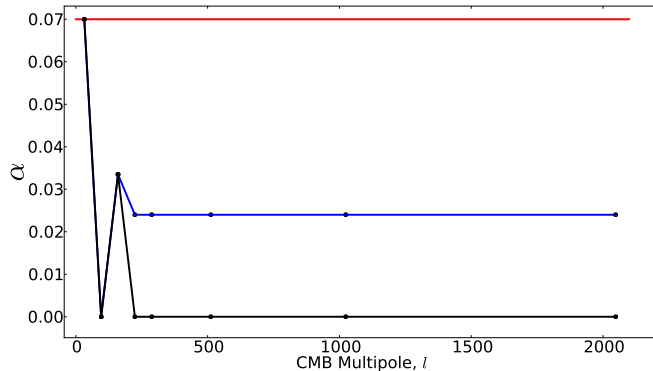


Figure 1. The profiles of amplitude of modulation for the three different cases studied in the present work - (i) SD-1 : a scale dependent modulation profile with some residual anisotropy at small scales, (ii) SD-2 : scale dependent profile as seen in PLANCK data, and (iii) SID : a scale independent modulation, are shown here in blue, black and red respectively.

show, three kinds of modulation profiles considered in the present work viz., (i) a scale dependent (SD-1) modulation strength depicted by blue curve with some residual power at high l , (ii) a scale dependent (SD-2) modulation strength depicted by black curve to mimic the observed profile in PLANCK data [8, 9], and (iii) a scale independent (SID) modulation depicted by red curve in the same figure. Using the BipoSH coefficients for these two different cases, we produce nSI Gaussian simulations as described in the next section.

3 Simulations

To study the effect of dipole power asymmetry on cosmological parameters, we produce dipole modulated CMB skies at HEALPix¹ [39] resolution parameter of $N_{side} = 1024$ using CoNIGS (Code for Non-Isotropic Gaussian Sky). CoNIGS is a numerical algorithm developed by Mukherjee & Souradeep [38] to produce statistically anisotropic Gaussian realizations of CMB. This algorithm implements Cholesky decomposition of the covariance matrix, $K_{lml'm'}$ in Eq. 2.2 which contains both angular power spectra C_l and BipoSH coefficients $A_{ll'}^{1N}$, and obtains the corresponding lower triangular matrix. Operating this lower triangular matrix on an array of random draws from a unit variance Gaussian distribution produces the simulations which have inherently broken statistical isotropy with given BipoSH spectra as ensemble mean. With input as angular power spectra (consistent with PLANCK) and BipoSH coefficients due to CHA, we generate nSI Gaussian simulations for our analysis.

Simulations with both scale dependent and scale independent modulation amplitudes as shown in Fig. 1, are generated. These simulations are free from any foreground contamination, instrumental noise and asymmetric beam. Hence this analysis is not affected by any systematics. The corresponding isotropic simulations are produced with the same seed and theoretical C_l , used to produce nSI simulations. To study the effect of statistical anisotropy on cosmological parameters, we need to extract the angular power spectrum, C_l , from different sky directions. We divide the sky into mutually exclusive partitions as shown in Fig. 2.

¹<http://healpix.jpl.nasa.gov/>

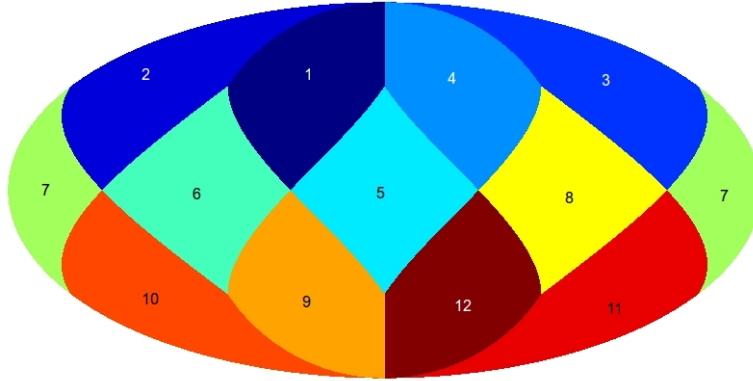


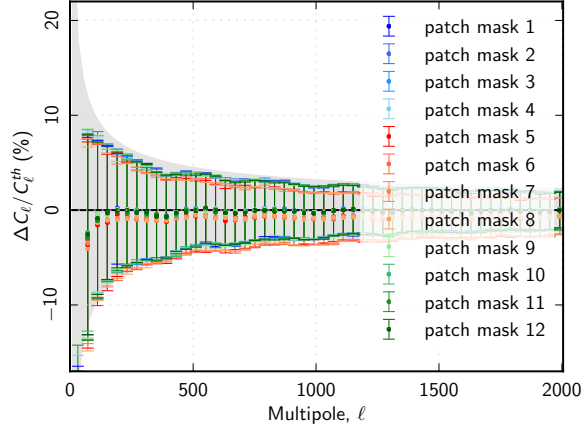
Figure 2. Full sky realizations of CMB are partitioned into 12 different regions as depicted in this diagram. Cosmological parameters are estimated from these 12 different patches from SI and nSI simulations. The anisotropic simulations are produced with cosmic hemispherical asymmetry injected in the direction of pixel center of patch 12.

To assess the maximum effect induced by isotropy violation on cosmological parameters, we inject the CHA in the direction of one of the pixel centers of `HEALPix` $N_{side} = 1$ grid, which are our sky partitions shown in Fig. 2. Specifically we choose pixel center corresponding to patch 12 as the direction for injecting dipole modulation in our simulations. The pseudo- C_l MASTER algorithm [40] is used to recover angular power spectrum from each of these patches in the multipole range $l = [2, 2048]$ using a bin width of $\Delta l = 20$. Due to the limited size of these sky patches, the recovered C_l are more accurate at high ‘ l ’ as shown in Fig. 3(a). To avoid artefacts due to sharp boundaries of the sky partitions in C_l recovery, we anodise each partition shown in Fig. 2 with a Gaussian beam of FWHM=50’ (arcmin) and requiring $\beta \sim 10^{-3}$ following [41]. The estimated C_l from the central patches (5, 6, 7, 8) shows a mild under estimate of power. However, the recovered C_l are completely consistent within the cosmic variance as shown in Fig. 3(a). The covariance matrix of the binned C_l obtained from 1000 SI simulations with a bin width of $\Delta l = 20$, from the patch 12, is shown in Fig. 3(b). It is defined as $C_{ij} = \langle \delta C_{l_i} \delta C_{l_j} \rangle / \sqrt{\langle \delta C_{l_i}^2 \rangle \langle \delta C_{l_j}^2 \rangle}$, where $\delta C_{l_i} = C_{l_i} - \langle C_{l_i} \rangle$ and C_{l_i} is the recovered angular power spectrum from partial sky from the multipole bin ‘ i ’. The range of multipoles that correspond to bin i are $[(i - 1) * \Delta l + 2, i * \Delta l + 1]$, and l_i denotes the central multipole of this bin. We also checked the covariance matrices of the recovered C_l from other sky partitions, and find them to be predominantly diagonal.

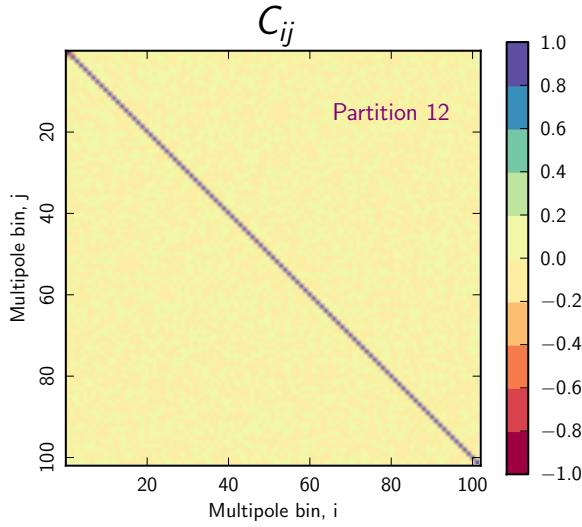
Due to SI violating dipole modulation, C_l recovered from different patches would differ for SI and nSI simulations, which in turn affect the cosmological parameters from them. In our analysis, we don’t consider C_l recovered at low multipoles $l = [2, 41]$ for estimating the cosmological parameters estimation for SID and SD-1 case. For SD-2 case the effect of modulation is present only at low l , so we consider the full range of $l = [2, 2048]$ in our analysis. In the next section, we discuss the results for the four different cases.

4 Assessing directional dependence of cosmological parameters

From the angular power spectra obtained from the 12 sky partitions, we estimate cosmological parameters for all the four cases : SI (statistical isotropy), SD-1 (scale dependent with some constant power at high l), SD-2 (scale dependent with no power at high l) and SID (Scale



(a)



(b)

Figure 3. (a) Percent difference plot of the recovered mean C_l with error bars from different patches of 1000 SI simulations in comparison to the input theoretical C_l used to generate the simulations. The convergence to the injected C_l improves with l and are well within the cosmic variance $= \sqrt{2/(2l+1)} \times 100(\%)$. (b) The covariance matrix of binned C_l obtained from 1000 simulations from mask region 12 is shown here. Bin index ‘ i ’ contains the multipoles $[(i-1) * \Delta l + 2, i * \Delta l + 1]$, where $\Delta l = 20$ is the chosen bin width. One can clearly see that the covariance matrix is sufficiently diagonal.

independent). As these ideal simulations are free from any instrumental noise or systematics, the variance of angular power spectra is solely due to cosmic variance. As a result, we can define the likelihood as

$$-\log \mathcal{L}(C_l | \bar{C}_l) = \sum_{l'} (C_l - \bar{C}_l) G_{l'}^{-1} (C_l - \bar{C}_l)^T, \quad (4.1)$$

where, $G_{l'}$ denotes the signal cosmic covariance matrix for C_l . In our case, $G_{l'}$ is a diagonal matrix containing only cosmic variance. C_l indicates the model power spectra while \bar{C}_l indicates the recovered power spectrum from different patches.

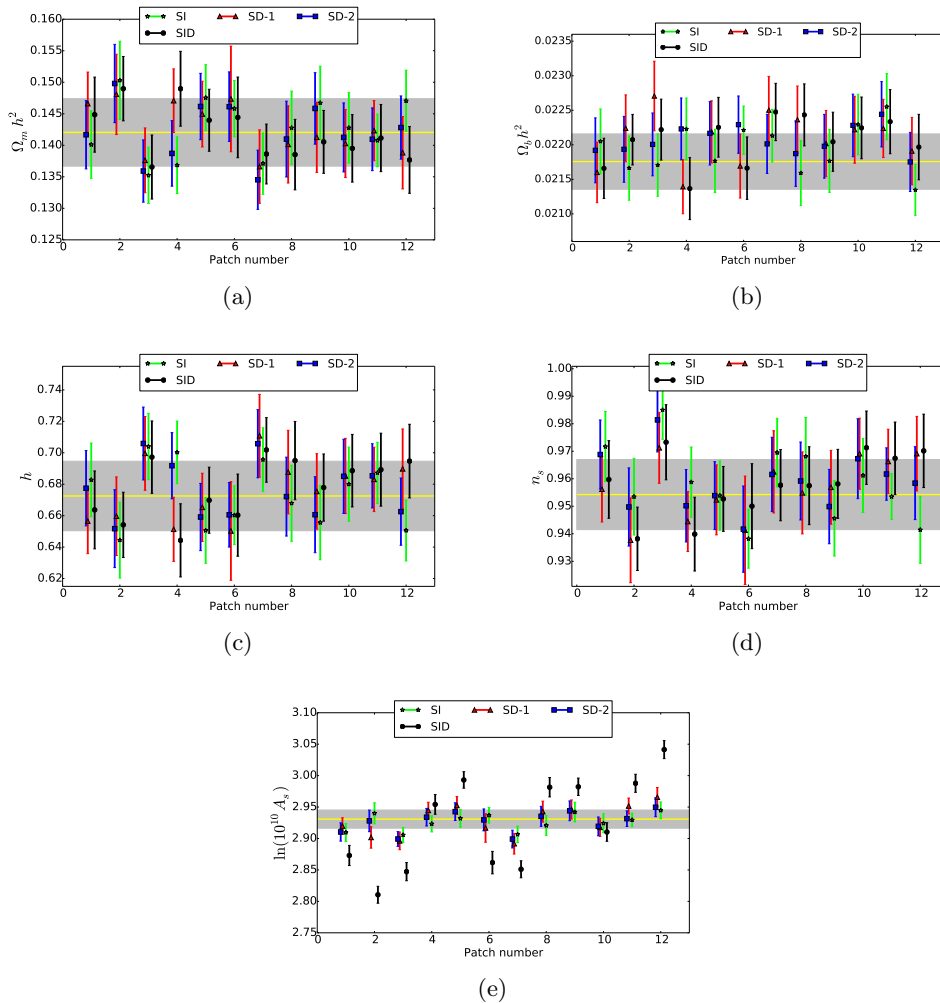


Figure 4. The mean and standard deviation of the best-fit cosmological parameters $\{\Omega_m h^2, \Omega_b h^2, h, n_s, A_s\}$ (τ is excluded) obtained from the 12 sky partitions (shown in Fig. 2) of a single realization that is (i) Statistically Isotropic (SI) (green), (ii) anisotropic with scale independent (SID) modulation profile (black), (iii) anisotropic with SD-1 profile (red), and (iv) anisotropic with SD-2 profile (SID, SD-1 and SD-2 dipole modulation profiles are shown in Fig. 1). In grey, we show the 1σ region for each parameter estimated from the full sky SI simulation with the mean depicted in yellow. Same seed is used to generate all the four CMB sky maps viz., SI, SID, SD-1, SD-2 to allow direct comparison of the derived cosmological parameters. None of the parameters, except for the scalar amplitude A_s , show any significant variation with sky direction, in comparison to that arising due to cosmic variance in a statistically isotropic model.

From the nSI maps produced with SD-1, SD-2 and SID modulation profiles, we obtain the best-fit standard model cosmological parameters $\{\Omega_m h^2, \Omega_b h^2, h, \tau, n_s, A_s\}$, from all partitions of the sky using SCoPE (Slick Cosmological Parameter Estimator), developed by Das & Souradeep [42]. We also obtain the same set of six cosmological parameters from all the 12 patches from the corresponding SI simulation with the same seed. The parameter estimation uses C_l in the range $l = [40, 2048]$ for SI, SD-1 and SID case and $l = [2, 2048]$ for SD-2 case. Since we limit to only temperature data, τ cannot be constrained by this analysis.

A comparison of the estimated cosmological parameters from various patches are de-

Table 1. Summary on departure of cosmological parameters due to dipole power asymmetry (in units of σ) as seen in n SI case compared to full sky SI case.

Parameter	Maximum relative departure seen in SD-1 case	Maximum relative departure seen in SD-2 case	Maximum relative departure seen in SID case	Remarks
A_s	2.27σ for patch 12 and 1.7σ for patch 2	1.25σ for patch 12 and 0.16σ for patch 2	7.71σ for patch 12 and 8.93σ for patch 2	Important for SID. Not significant for SD-1 and SD-2.
n_s	1.1σ for patch 12	0.31σ for patch 12	1.19σ for patch 12	Not significant. Indicates a mild increase (or decrease) in the direction (or opposite) of cosmic hemispherical asymmetry.
h	1.04σ for patch 4	0.9σ for patch 4	1.21σ for patch 4	Not significant
$\Omega_m h^2$	0.93σ for patch 4	1.06σ for patch 4	0.87σ for patch 4	Not significant
$\Omega_b h^2$	0.94σ for patch 2	1.23σ for patch 2	1.36σ for patch 2	Not significant

pictured in Fig. 4 for SI (green), SD-1 (red), SD-2 (blue) and SID (black) cases from a single CMB realization with same seed. The use of same seed for generating an SI map as well as n SI maps with SID, SD-1 and SD-2 modulation profiles, allows us to understand the directional dependence in the inferred cosmological parameters corresponding to each of these SI violation scenarios.

In this figure, we plotted the mean along with 1σ variation of all the five parameters, derived from posteriors constructed using SCoPE chains, as a function of sky partition number. As can be seen from Fig. 4, the maximum discrepancy is observed for the parameter A_s . A large positive departure from the SI simulation estimate is evident only in patch 12, for SID case, as this is the direction of the injected dipole power asymmetry. Correspondingly a large negative shift for A_s is seen in the direction of patch 2. All other patches adjacent to patch numbers 12 and 2 also show a drift towards higher and lower value of A_s , respectively. Estimates from patch number 10 and 4 do not show any notable departure. On comparison, for a 7% amplitude of dipole modulation in SD-1 and SD-2 cases at low l , the recovered parameters are found to be completely consistent with SI map within 1.5σ . SID case shows a severe departure as expected. But PLANCK-2015 results [9] clearly indicate that, the amplitude of observed dipole modulation falls off beyond $l \sim 64$.

In Table 1, we list the discrepancy between cosmological parameters derived from SID, SD-1 and SD-2 cases, individually in comparison to the parameters estimated from full sky SI map (except for τ which cannot be constrained using only temperature data). It is also important to note that, although the departure of n_s in any of the patches from SI case is at best $\sim 1.2\sigma$, there is a clear trend of excess/deficit in the same/opposite direction of dipole power asymmetry. In the hemisphere with more fluctuations, n_s indicates a mild increase

for the SID modulation case, whereas in the opposite hemisphere there is a reduction in its value. This is opposite to the trend observed by Axelsson et al. [33] in the WMAP data. If a similar behaviour is observed for n_s in PLANCK data, then it may have an origin different from CHA. It may well be due to foreground contamination. Nevertheless, these estimates of n_s from different patches/sky directions for both SD and SID cases are in good agreement with those derived from full sky SI map.

To understand the statistical nature of the nSI signal, we estimate the excess (deficit) power in the direction \hat{p} , i.e., towards the center of patch 12 (in $-\hat{p}$ direction which corresponds to center of patch 2) from 1000 simulations using local variance estimator proposed by Akrami et al. [13]. Histogram of recovered dipole amplitudes from the normalized variance variation maps ($\xi(\hat{N})$) in both directions, obtained from each of the 1000 nSI maps corresponding to SD-2 and SID cases are plotted in figure Fig. 5(a) and Fig. 5(b), respectively. A brief description of this procedure is given in Appendix A. From Fig. 5(b), we see that the mean of the recovered dipole amplitudes in \hat{p} and $-\hat{p}$ directions of variance variation maps thus obtained from simulations match with the injected amplitude $2A = 0.14$. The histogram also indicates that there are many simulations with much lower dipole amplitude than 0.14. Hence the estimated parameters, particularly A_s , from a given map/realization can be smaller than 14% in the direction of anisotropy as was found here. In the SID case, we find only a 4% excess (deficit) in A_s in patch 12 (patch 2) which is within 1σ of the mean dipole amplitude obtained from 1000 simulations as shown in Fig. 5(b). A similar effect is also observed in the SD-1 case which has a residual dipole anisotropy of $\sim 2.5\%$ in amplitude at high l . We find that the estimated value of A_s from patch 12 from the specific realization we used is also lower (than 5%), but within 1σ of the dipole amplitude distribution shown in Fig. 5(a). Thus we can understand this recovery of lower value for A_s than the expected/injected value along the axis of dipole modulation (i.e., from sky partitions 12 and 2) as a manifestation of the statistical nature of the underlying anisotropic signal.

Using WMAP data, Axelsson et al. [33] also found a mild direction dependence for $\Omega_b h^2$. But our analysis on ideal simulations that compares nSI map with corresponding SI map does not show any such departure and hence does not have any discernible pattern for $\Omega_b h^2$ due to CHA.

Other parameters does not show any significant departure or special trend in comparison to the SI case. This is similar to the finding by [33] using WMAP data. All other parameters shows variations which are well within 1σ of the SI simulation and doesn't show any variation. To summarize, the current analysis indicates that the presence of dipole power asymmetry at an amplitude of 7% seem to affect the cosmological parameters related to inflationary physics i.e., A_s and n_s . Rest of the parameters appear to be not influenced by its presence.

5 Conclusion

The estimation of cosmological parameters from noise and foreground free dipole modulated statistically non-isotropic (nSI) simulations allows an assessment of the maximum possible departure that can arise in such a nSI map, in comparison to their estimates from a corresponding statistically isotropic (SI) sky. For several partial sky missions of CMB and other cosmological/astrophysical missions with limited sky coverage, it is essential to be aware of any departure in the parameters compared to SI model. Our analysis sheds light on this specific issue by estimating the cosmological parameters from sky partitions in different directions, and identifies the parameters most susceptible to the presence of a dipolar modulation

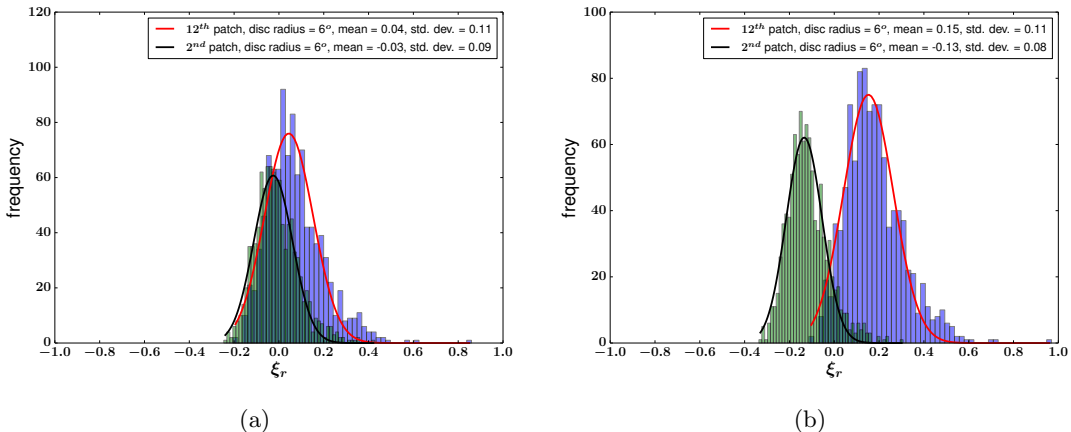


Figure 5. Histogram of dipole amplitudes recovered from \hat{p} and $-\hat{p}$ directions of the normalized variance variation maps, $\xi(\hat{N})$, obtained from 1000 nSI maps injected with (a) SD-2 and (b) SID modulation profiles. The distributions are overlaid with a Gaussian function with the mean and standard deviation mentioned in the plot.

SI violation. We perform the estimation in the 12 different sky partitions shown in Fig. 2 using nSI and corresponding SI simulation. The nSI simulations are produced using CoNIGS algorithm with dipole modulation that is scale dependent (as observed by PLANCK), as well as, the simpler scale independent amplitude profiles as shown in Fig. 1. The injected direction for the modulation in both the cases is taken to be the center of the patch mask 12 from Fig. 2, to maximize the effect of SI violation and amplitude is taken to be 0.07 consistent with that indicated in the recent PLANCK cosmological results.

The parameter that is most susceptible to variation on the sky due to SI violation is A_s . As expected, it clearly predicts a higher value in the direction of modulation and a lower value in the opposite direction. Variations as large as 7.7σ and 8.93σ deviations are observed in A_s from patches 12 and 2, respectively, for SID case. However, for the SD-2 model, which mimics the observed modulation profile in CMB maps from PLANCK observations, only a 1.25σ deviation is seen in patch 12. This indicates that the estimates from SD-2 model would not differ significantly from those obtained from a full sky SI map. However, if the scale dependent modulation is extended to high l as in SD-1 case, then a 2.27σ and 1.7σ departures were seen in the sky directions 12 and 2, respectively, in comparison to the SI map estimates. This is due to the fact that the cosmological parameters are heavily influenced by C_l at high l , rather than low l power spectrum. The other parameter that is found to be mildly susceptible to SI violation is n_s . It does not show any significant departure in simulations with SD-1, SD-2 and SID modulation profiles compared to SI case. But it indicates a higher value in the direction of CHA than in the opposite direction. Rest of the parameters do not show any significant variation correlated with the presence of CHA. In essence, the inflationary parameters, A_s and n_s , are found to be more susceptible to change with direction than other parameters, due to dipole power asymmetry.

In summary, we conclude that the base LCDM model parameters does not show any direction dependence, as long as the modulation amplitude of 7% is scale dependent and is present only at large angular scales ($> 3^\circ$) [8, 9]. The determination of the true nature of CHA from future analysis [45], can give a better estimate on the effect of A_s and n_s .

Our local motion through CMB rest frame ($\vec{\gamma} = \vec{v}/c$) also induces (a scale independent) SI violation [46–48] with a magnitude of $\mathcal{M} \equiv |\gamma| = 0.00123$ [49], that is much weaker than the modulation strength considered here. As a result, all the cosmological parameters can be safely considered to be unaffected by Doppler boosting of CMB anisotropies. Future CMB and other cosmological surveys from diverse observational windows may reveal the true origin/extent of this observed CHA in CMB. Recently, an analysis on Lyman- α forest [50] from $z > 2$ quasar data set of SDSS-III BOSS DR9 indicates no significant ($> 3\sigma$) departures from SI model. A similar study on SNIa was also carried out recently [51]. The current analysis using simulated ideal nSI maps will be useful in carefully inferring evidence for direction dependent cosmological parameters from those observations.

Acknowledgement : S. Mukherjee and S. Das thanks Council of Scientific & Industrial Research (CSIR), India for financial support as Senior Research Fellows. S. Shaikh thanks University Grants Commission (UGC), India for providing the financial support as Senior Research Fellow. The present work is carried out on the High Performance Computing facility at IUCAA. The authors acknowledge the use of MASTER routine from the Cosmology Routine Library in Fortran (CRL) webpage of E. Komatsu (<http://www.mpa-garching.mpg.de/~komatsu/crl/>).

A Local Variance Estimator

CHA leads to asymmetry in variances computed locally on a CMB temperature map. This relation between CHA and local variances was used by Akrami et al. [13] to obtain the amplitude (A) and direction (\hat{p}) of the low l hemispherical asymmetry modelled as dipole modulation of CMB anisotropies. The local variance $\sigma_r^2(\hat{N})$ in the direction \hat{N} refers to the variance of temperature map computed using pixels falling within a circular disc of a chosen radius ‘ r ’ centred at \hat{N} i.e.,

$$\sigma_r^2(\hat{N}) = \sum_{\hat{n} \in r} (T(\hat{n}) - T_r(\hat{N}))^2, \quad (\text{A.1})$$

where $T_r(\hat{N})$ is the mean of all pixels inside the radius ‘ r ’ of the circular disc defined at \hat{N} . In practice, a local variance map is obtained from a temperature map at higher resolution with HEALPix resolution parameter $\mathbf{nside} = N_{side,high}$, using a low resolution HEALPix grid with $\mathbf{nside} = N_{side,low}$ ($< N_{side,high}$). The low resolution HEALPix grid is used to define the disc centres \hat{N} at which we compute the local variances. The variances thus computed locally at \hat{N} are assigned as pixel values to the corresponding HEALPix pixel indices, to obtain a local variance map at $\mathbf{nside} = N_{side,low}$.

When computing local variances in real data, one has to use an effective disc obtained by multiplying the circular disc of radius ‘ r ’ defined locally at the sky position \hat{N} and the galactic mask so as to avoid biases due to foreground contamination. Since less number of pixels will be available in the net disc, one can impose an additional criteria of using that location in fitting the dipole signal only if at-least 50% (for example) of pixels are available for computing the local variance, after taking the union of circular disc defined at that location and the galactic mask, compared to the total number of pixels available in the full disc of radius ‘ r ’. For a dipole modulated map given by Eq. 2.3 which is otherwise isotropic, local variances are related by $\tilde{\sigma}^2(\hat{N}) \approx (1 + 2\alpha \hat{p} \cdot \hat{N})\sigma^2(\hat{N})$, where $\tilde{\sigma}^2$ and σ^2 denote local variances corresponding to modulated and unmodulated CMB sky respectively (computed using a circular disc of chosen radius ‘ r ’ centred in the sky direction \hat{N}). Thus, in order to

obtain a correct estimate of the dipole signal lying beneath the observed sky, we define a normalized variance variation map as

$$\xi_r(\hat{N}) = \frac{\tilde{\sigma}_r^2(\hat{N}) - \langle \sigma_r^2(\hat{N}) \rangle}{\langle \sigma_r^2(\hat{N}) \rangle}, \quad (\text{A.2})$$

where $\langle \sigma_r^2(\hat{N}) \rangle$ denotes mean variance map obtained from an ensemble of SI simulations. By fitting a dipole to this normalized variance map, ξ_r , the direction (\hat{p}) and strength (A) of modulation signal present in a given map can be recovered.

Here we assess the statistical nature of the anisotropic signal underlying an nSI map, by reading the pixel values of $\xi_r(\hat{N})$ in \hat{p} and $-\hat{p}$ directions. For the SID modulation case, we expect to find $\langle \xi_r(\hat{p}) \rangle = \langle \xi_r(-\hat{p}) \rangle = 2A$. In the case of an nSI map with scale dependent modulation amplitude, the angular dependence of the intrinsic modulation strength can be profiled by estimating $\xi_r(\hat{N})$ for different choices of disc radii ‘ r ’ and obtaining its dipole component thereof.

References

- [1] P. A. R. Ade et al., *Planck 2013 results. XV. CMB power spectra and likelihood*, *Astron. Astrophys***571** (2014) A15.
- [2] P. A. R. Ade et al., *Planck 2013 results. XVI. Cosmological parameters*, *Astron. Astrophys* **571**, (2014) A16.
- [3] N. Aghanim et al., *Planck 2015 results. XI. CMB power spectra, likelihoods, and robustness of parameters*, *arXiv:1507.02704* (2015).
- [4] P. A. R. Ade et al., *Planck 2015 results. XIII. Cosmological parameters*, *arXiv:1502.01589* (2015).
- [5] C. L. Bennett et al., *Nine-year Wilkinson Microwave Anisotropy Probe (WMAP) Observations: Final Maps and Results*, *ApJS*, **208**, **20B**, (2013)
- [6] H. K. Eriksen et al., *Hemispherical Power Asymmetry in the Third-Year Wilkinson Microwave Anisotropy Probe Sky Maps*, *ApJ*, **660**, **L81**, (2007)
- [7] J. Hoftuft et al., *Increasing evidence for hemispherical power asymmetry in the five-year WMAP data*, *ApJ*, **699**, **985**, (2009)
- [8] P. A. R. Ade et al., *Planck 2013 results. XXIII. Isotropy and statistics of the CMB*, *A&A*, **571**, **A23**, (2014)
- [9] P. A. R. Ade et al., *Planck 2015 results. XVI. Isotropy and statistics of the CMB*, *arXiv:1506.07135*, (2015)
- [10] F. K. Hansen, A. J. Banday & K. M. Gorski, *Testing the cosmological principle of isotropy: local power spectrum estimates of the WMAP data*, *MNRAS*, **354**, **641**, (2004)
- [11] H. K. Eriksen et al., *Asymmetries in the Cosmic Microwave Background Anisotropy Field*, *ApJ*, **605**, **14**, (2004)
- [12] F. Paci et al., *Hemispherical power asymmetries in the WMAP 7-year low-resolution temperature and polarization maps*, *MNRAS*, **434**, **3071**, (2013)
- [13] Y. Akrami et al., *Power asymmetry in WMAP and Planck temperature sky maps as measured by a local variance estimator*, *ApJ*, **784**, **L42**, (2014)
- [14] M. Quartin & A. Notari, *On the significance of power asymmetries in Planck CMB data at all scales*, *JCAP*, **01**, **008**, (2015)

- [15] A. L. Erickcek, M. Kamionkowski & S. M. Carroll, *A hemispherical power asymmetry from inflation*, *Phys.Rev. D* **78**, 123520, (2008)
- [16] A. L. Erickcek, S. M. Carroll & M. Kamionkowski, *Superhorizon perturbations and the cosmic microwave background*, *Phys. Rev. D*, **78**, 083012, (2008)
- [17] J. F. Donoghue, K. Dutta, & A. Ross, *Nonisotropy in the CMB power spectrum in single field inflation*, *Phys.Rev. D* **80**, 023526, (2009)
- [18] L. Dai, D. Jeong, M. Kamionkowski & J. Chluba, *The pesky power asymmetry*, *Phys. Rev. D*, **87**, 123005, (2013)
- [19] D. H. Lyth, *Generating f_{nl} at $\ell \sim 60$* , *JCAP*, **04**, 039, (2015)
- [20] J. McDonald, *Hemispherical power asymmetry from a space-dependent component of the adiabatic power spectrum*, *Phys. Rev. D*, **89**, 127303, (2014)
- [21] A. A. Abolhasani, S. Baghram, H. Firouzjahi & M. H. Namjoo, *Asymmetric sky from the long mode modulations*, *Phys. Rev. D*, **89**, 063511, (2014)
- [22] M. H. Namjoo, A. A. Abolhasani, S. Baghram & H. Firouzjahi, *CMB Hemispherical Asymmetry: Long Mode Modulation and non-Gaussianity*, *JCAP*, **08**, 002, (2014)
- [23] S. Jazayeri, Y. Akrami, H. Firouzjahi, A. R. Solomon & Y. Wang, *Inflationary power asymmetry from primordial domain walls*, *JCAP*, **11**, 044, (2014)
- [24] J. Chluba, L. Dai, D. Jeong, M. Kamionkowski & A. Yoho, *Linking the BICEP2 result and the hemispherical power asymmetry through spatial variation of r* , *MNRAS*, **442**, 670, (2014)
- [25] S. Mukherjee, *Hemispherical asymmetry from an isotropy violating stochastic gravitational wave background*, *Phys. Rev. D*, **91**, 062002, (2015)
- [26] R. Kothari, P. K. Rath & P. Jain, *Imprint of Inhomogeneous and Anisotropic Primordial Power Spectrum on CMB Polarization*, *arXiv:1503.03859*, (2015)
- [27] R. Kothari et al., *Cosmological Power Spectrum in Non-commutative space-time*, *arXiv:1503.08997*, (2015)
- [28] S. Mukherjee & T. Souradeep, *CMB power asymmetry and suppression: Two sides of the same coin*, *arXiv:1504.02285*, (2015)
- [29] Z. Kenton, D. J. Mulryne & S. Thomas, *Generating the cosmic microwave background power asymmetry with g_{NL}* , *Phys. Rev. D* **92**, 023505, (2015)
- [30] A. Ashoorioon & T. Koivisto, *Hemispherical Asymmetry from Parity-Violating Excited Initial States*, *arXiv:1507.03514*, (2015)
- [31] S. Adhikari, S. Shandera, A. L. Erickcek, *Large-scale anomalies in the cosmic microwave background as signatures of non-Gaussianity*, *Phys. Rev. D* **93**, 023524, (2016)
- [32] Y. F. Cai, D. G. Wang, W. Zhao, Y. Zhang, *Scale-dependent CMB power asymmetry from primordial speed of sound and a generalized δN formalism*, *JCAP* **02**, 019, (2016)
- [33] M. Axelsson et al., *Directional dependence of Λ CDM cosmological parameters*, *ApJ*, **773**, L3, (2013)
- [34] A. Hajian & T. Souradeep, *Measuring the Statistical Isotropy of the Cosmic Microwave Background Anisotropy*, *ApJ*, **597**, L5, (2003)
- [35] S. Basak, A. Hajian & T. Souradeep, *Statistical isotropy of CMB polarization maps*, *Phys. Rev. D*, **74**, 021301, (2006)
- [36] C. Gordon, *Broken Isotropy from a Linear Modulation of the Primordial Perturbations*, *ApJ*, **656**, 636, (2007)

- [37] C. Gordon & R. Trotta, *Bayesian calibrated significance levels applied to the spectral tilt and hemispherical asymmetry*, *MNRAS*, **382**, 1859, (2007)
- [38] S. Mukherjee & T. Souradeep, *Statistically anisotropic Gaussian simulations of the CMB temperature field*, *Phys. Rev. D*, **89**, 063013, (2014)
- [39] K. M. Gorski et al., *HEALPix: A Framework for High-Resolution Discretization and Fast Analysis of Data Distributed on the Sphere*, *ApJ*, **622**, 759, (2005)
- [40] E. Hivon et al., *MASTER of the Cosmic Microwave Background Anisotropy Power Spectrum: A Fast Method for Statistical Analysis of Large and Complex Cosmic Microwave Background Data Sets*, *ApJ*, **567**, 2, (2002)
- [41] J. Kim, *How to make a clean separation between CMB E and B modes with proper foreground masking*, *A&A*, **531**, A32, (2011)
- [42] S. Das & T. Souradeep, *SCoPE: An efficient method of Cosmological Parameter Estimation*, *JCAP*, **07**, 018, (2014)
- [43] A. G. Riess et al., *A 3% Solution: Determination of the Hubble Constant with the Hubble Space Telescope and Wide Field Camera 3*, *ApJ*, **730**, 119, (2011)
- [44] G. Efstathiou, *H₀ revisited*, *MNRAS*, **440**, 1138, (2014)
- [45] S. Mukherjee & T. Souradeep, *Litmus Test for Cosmic Hemispherical Asymmetry in the Cosmic Microwave Background B-mode polarization*, *Phys. Rev. Lett.* **116**, 221301, (2016)
- [46] A. Kosowsky & T. Kahniashvili, *Signature of Local Motion in the Microwave Sky*, *Phys. Rev. Lett.*, **106**, 191301, (2011)
- [47] L. Amendola et al., *Measuring our peculiar velocity on the CMB with high-multipole off-diagonal correlations*, *JCAP*, **07**, 027, (2011)
- [48] S. Mukherjee, A. De & T. Souradeep, *Statistical isotropy violation of CMB Polarization sky due to Lorentz boost*, *Phys. Rev. D*, **89**, 083005, (2014)
- [49] A. Kogut et al., *Dipole Anisotropy in the COBE DMR First-Year Sky Maps*, *ApJ*, **419**, 1, (1993)
- [50] D. K. Hazra & A. Shafieloo, *Search for a direction in the forest of Lyman- α* , *JCAP*, **11**, 012, (2015)
- [51] B. Javanmardi et al., *Probing the isotropy of cosmic acceleration traced by Type Ia supernovae*, *ApJ*, **810**, 47J, (2015)